34th EPS Conference on Plasma Phys. Warsaw, 2 - 6 July 2007 ECA Vol.**31F**, P-4.069 (2007)

Modeling of MHD Events during Pellet-Plasma Interaction in Tokamak

A.A.Ivanov[1], A.A.Martynov[1], S.Yu.Medvedev[1],

D.A.Kislov[2], B.V.Kuteev[2], V.D.Pustovitov[2] and A.M.Popov[3]

[1]*Keldysh Institute, Russian Academy of Sciences, Moscow, Russia*

[2]*Nuclear Fusion Institute, Russian Research Center "Kurchatov Institute", Moscow, Russia*

[3]*Moscow State University, Moscow, Russia*

The MHD-events initiated by pellets may significantly contribute to faster and deeper penetration of the pellet matter into the plasma. In particular, the threshold effect of the pellet size for appearance of the ablation bursts and drops in the T-10 experiments provides the experimental evidence for that [1].

The processes of pellet-plasma interaction require integrated modeling including the pellet ablation model, 3D MHD and anisotropic transport. The present study initiates the step-by-step mathematical modeling of the processes involved. The pellet penetration is modeled by the axisymmetric cooling wave propagation. During that quasi-equilibrium process, the MHD mode destabilization can take place due to the plasma conductivity drop and the current density layer formation at the cooling front.

The effect of local plasma conductivity decrease on the nonlinear dynamics of the tearing modes was investigated using the nonlinear three-dimensional magnetohydrodynamic code NFTC [2]. The nonlinear modeling showed very fast growth of the magnetic islands when the cooling front passed the corresponding rational surface. The NFTC results for the axisymmetric cooling wave propagation were cross-checked with the quasi-equilibrium model using the 1.5D code SPIDER for simulation of the magnetic field diffusion and current density evolution in the moving front. The detailed structure of the quasi-stationary current density pulse was investigated under different assumptions about the temperature front shape. The linear stability analysis was performed for the series of equilibria. The ideal MHD modes were found to be stable even under artificially large localized perturbations of both shear and pressure gradient. On the other hand, the linear stability of the tearing modes was strongly affected even by minor safety factor perturbations.

1 NTM excitation by pellet propagation

The numerical modeling of the pellet injection and the excitation of the neoclassical tearing modes (NTM) was performed using the nonlinear 3D code NFTC. The cooling front resulting from the pellet penetration is investigated using the model of the moving localized perturbation of the plasma conductivity and density. The change of the conductivity near the resonant surface leads to the toroidal current density perturbation. The current density perturbation results in an increase of the tearing mode stability parameter Δ', which is negative for the initial equilibrium. As the value of Δ' increases, the threshold for the NTM stability decreases driving the NTMs unstable. The growth rate of the NTM mode is much larger in this case compared to the usual NTM mode growth rate that is determined by low bulk plasma resistivity. The spatial localization of the conductivity perturbation is of the same magnitude as the seed island width for the NTM. So the effect of local conductivity change near the resonant surface during the pellet passing is the cause of the NTM destabilization. Magnetic islands created during the pellet crossing of resonant magnetic surfaces can be seed islands for further instability growth.

The MHD equilibrium used corresponds to the ITER inductive scenario 2 but the plasma parameters are changed to the T-10 characteristic values. The pellet size in the T-10 experiments varied between 0.2 mm and 0.6 mm. The velocity of pellet is about 400 m/s, averaged density $< n_e >= 10^{13}$ cm^{-3}, electron temperature T_e=1.2 keV, plasma current I_p=270 kA, magnetic field B_t=2.4 T, minor radius a=30 cm.

Outside perturbation region the bulk plasma resistivity was taken to correspond to the magnetic Reynolds number 10^{-7}. The perturbation width was taken to be 0.0195a (6 mm for T-10) or 0.039a (12 mm for T-10) and the resistivity inside the colder zone was chosen 1000 times higher than in the bulk plasma.

In Fig.1 the destabilization of the mode $m/n = 3/2$ due to the resistivity perturbation is presented. For comparison, the evolution of the same parameters is shown for the case without the perturbation. The island growth rate is much higher for the case with perturbation compared to the conventional NTM. It is accompanied by the sharp growth of the Δ' parameter. The island growth rate is higher for larger pellet.

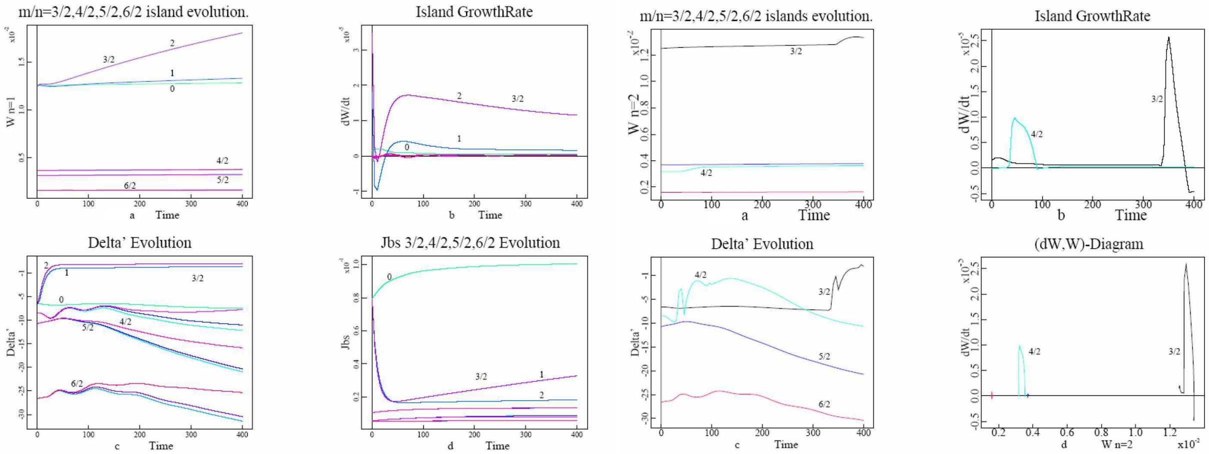

Fig.1 Time evolution of magnetic island width (a left), island growth rate (b left), stability parameter Δ' (c left) and bootstrap current (d left) for different sizes of pellet 6*mm (1),* 12*mm (2) and without resistivity perturbation (0). The time is given in Alfvén units.*
Excitation of the $n = 2$ NTMs with the moving front. Island width (a right), island growth rate (b right), stability parameter Δ' (c right) and the phase diagram $(\dot{W}, W)$ (d right)

The resistivity perturbation moving from the plasma boundary to the resonant surface $3/2$ results in the $4/2$ mode excitation first. Higher magnetic shear at the $q = 2$ surface gives smaller $4/2$ island and lower growth rate. Let us note that the islands remain almost unchanged after the front passing the resonant surface. The remaining islands can serve as seeds for the NTM if their size exceeds the corresponding threshold.

2 Quasi-equilibrium modeling of the cooling front

Small size of pellet, high conductivity and anisotropy of the diffusion coefficients in high temperature plasma make a full MHD solution quite a complicated task. The use of fast and reliable codes for quasi-equilibrium plasma evolution, ideal and resistive MHD stability makes possible interpretation of the results from the nonlinear codes, to determine the applicability limits and check the accuracy of the numerical experiments.

The propagation of the axisymmetric cooling wave that is not interacting with the magnetic islands is well described by 1.5D quasi-equilibrium plasma evolution taking into account the magnetic field diffusion. Such a model is implemented in the SPIDER code [3] and the detailed structure of the quasi-stationary perturbation of the current density is studied under different assumptions about the temperature in the front.

The unperturbed temperature profile is prescribed as a function of the square root of the normalized toroidal flux $a = \sqrt{\Phi/\Phi_b}$: $T_0(a) = T_b + (1-a^2)(T_a - T_b)$, where the values at the magnetic axis and the boundary for T-10 are chosen: $T_a = 1keV$, $T_b = 30eV$. The temperature drop at $a(t) = a_0 - v_{pellet}t$ moving with the velocity v_{pellet} in the flux variable a is given by the following relations:

$$T(a) = T_0(a(t) \pm w) + \left[1 - \left|\frac{a - a(t)}{w}\right|^p\right]^2 \left(T_{pellet} - T_0(a(t) \pm w)\right), \quad a \in [a(t), a(t) \pm w],$$

where w is the half-width of the colder zone. The parallel conductivity $\sigma_{||}$ is proportional to $T^{3/2}$.

In Fig.2 the evolution of the parallel current density, parallel component of the electric field, shear and conductivity are shown during about $100\mu s$ when the perturbation becomes quasi-stationary after the instant drop of the conductivity (initial front position $a_0 = 0.93$, the velocity v_{pellet} corresponds to $400m/s$, the exponent $p = 1$, $w = 0.005$ corresponds do the pellet diameter $3mm$ in T-10, $T_{pellet} = 5eV$) .

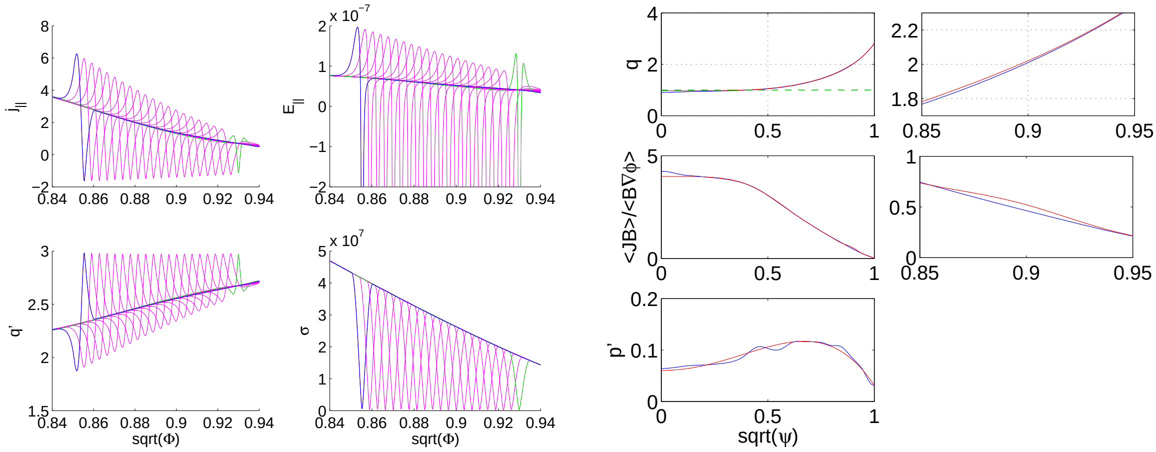

Fig.3 The evolution of the parallel current density, electric field, shear and conductivity in the moving front (left).
The original ASTRA and the smoothed profiles for the T-10 shot #42358 (right).

3 Ideal and tearing mode stability

The ASTRA simulation of the T-10 shot # 42358 gives the low-beta ($\beta_N = 0.3$) equilibrium that is stable against the $n = 1$ internal mode despite the safety factor at the magnetic axis below 1: $q_0 = 0.9$ (the instability takes place for $0.95 < q_0 < 1$).

However, linear tearing modes $m/n = 2/1$ and $3/2$ are unstable with the ASTRA profiles. A small change in the current density ($< 3\%$ of the current density at the axis) near the resonant surface $q = 2$ and smoothing of the plasma profiles makes the tearing modes stable (Fig.3).

The perturbation of the current density due to the temperature drop can drive the tearing mode unstable. In Fig.4 the tearing mode parameter Δ' and the normalized growth rates are plotted versus the position of the resonant surface $q = 2$ for the $m/n = 2/1$ mode. The tearing mode stability calculations were performed with the code DELTAPCYL [4].

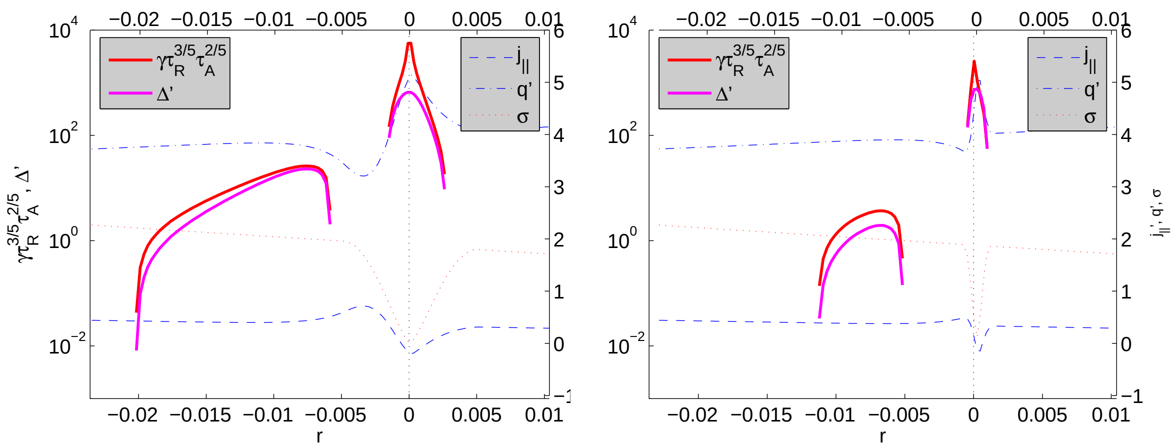

Fig.4 Growth rate of the 2/1 tearing mode versus the distance of the $q = 2$ resonant surface from the middle of the colder zone. Pellet diameter 3 mm (left) and 0.6 mm (right).

There are two regions of the tearing mode destabilization: ahead of the front (lower minor radii r in Fig.4) and inside the colder zone near the minimum of the temperature. In the first region the parameter Δ' and the growth rates are about two orders of magnitude lower. The stability gap between the two regions corresponds to the tearing mode stabilization due to the sharp drop in the current density. The mode becomes unstable again with sharp increase in both Δ' and growth rates when the resonant surface passes the point where the shear q'/q is minimal and enters the low temperature zone. Fig.4 also demonstrates that larger current density perturbation at the front for larger pellet size results in higher growth rates.

Lower values of $T_{pellet} = 1eV$ have a small effect on the growth rates (Fig.5, left). On the other hand, sharper temperature front (exponent $p = 2$) results in the increase of the current density perturbation and the growth rates for fixed pellet size (Fig.5, right).

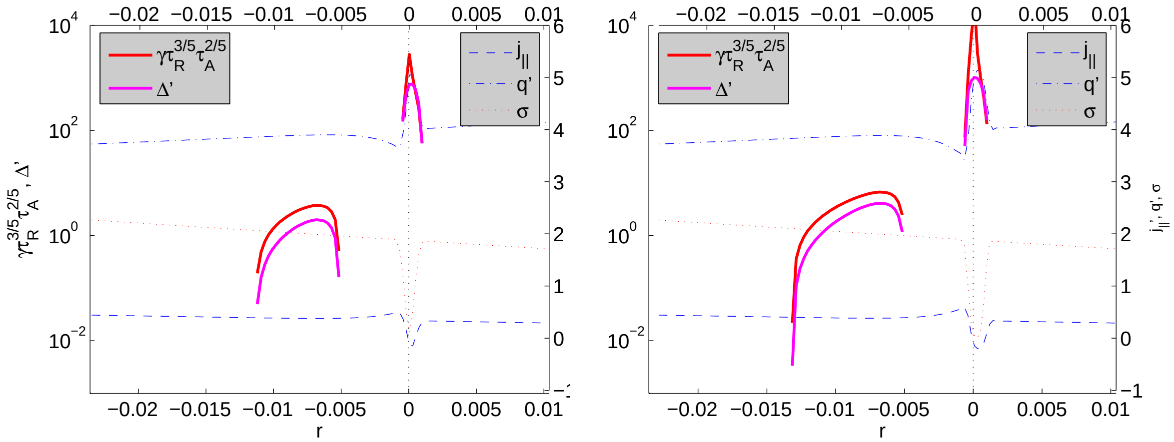

Fig.5 Growth rate of the 2/1 tearing mode versus the distance of the $q = 2$ resonant surface from the middle of the colder zone. Lower $T_{pellet} = 1eV$ (left). Sharper temperature front with $p = 2$, $T_{pellet} = 5eV$ (right). Pellet diameter 0.6 mm.

4 Conclusions

The computations performed with the 3D non-linear MHD code NFTC demonstrated the possibility of the excitation of the NTMs by the moving cooling front with the increased plasma resistivity due to the pellet penetration into plasma. The main mechanism of the tearing mode destabilization is related to the sharp increase of the Δ' parameter at the resonant surface of the corresponding mode. In turn, the significant increase in the Δ' values is related to the local toroidal current density perturbation propagating with the perturbed resistivity front.

The results of the NFTC computations were cross-checked for the axisymmetric cooling wave using the quasi-equilibrium evolution code SPIDER. The detailed computations of the magnetic field diffusion and current density evolution at the moving cooling front discovered the existence of the quasi-stationary distribution of the toroidal current density: the amplitude of the current density perturbation at the front is determined the size of the pellet and the sharpness of the temperature and resistivity drop; the perturbations dissipate at the trailing edge of the colder zone. The localized changes in the current density and safety factor profiles in tokamak plasma lead to strong increase of the tearing mode growth rates corresponding to the fast magnetic island growth in the nonlinear modeling.

The tearing mode stability calculations reveal an existence of the $\Delta' > 0$ zone ahead of the front. The width of the tearing unstable zone and the values of the growth rates depend on the pellet size.

The modeling is in qualitative agreement with the experimental data from the T-10 tokamak and confirms the interpretation of the results proposed in [1].

[1] B.V.Kuteev *et al.* JETP Letters, 2006, Vol.84, No.5, pp.239-242

[2] A.M.Popov. J.Plasma Physics, Vol.72, 2006, p.1101-1104

[3] A.A.Ivanov *et al.* Keldysh Institute of Applied Mathematics, Preprint No.7, Moscow, 2006 http : //www.keldysh.ru/papers/2006/source/prep2006_07.doc

[4] Ming Chu. Private communication. General Atomics, 1997
O.Sauter. Private communication. CRPP EPFL, 2007

Acknowledgement The authors are supported in part by the grant No.06-02-08224-obr of the Russian Foundation for Basic Research.